Available online at www.sciencedirect.com
SCIENCE DIRECT®
Journal of Crystal Growth 250 (2003) 83–89
JOURNAL OF CRYSTAL GROWTH
www.elsevier.com/locate/jcrysgro

# Growth and characterization of aliovalent ion-doped $LiCaAlF_6$ single crystals

Hiroki Sato[a,b,*], Hiroshi Machida[b], Martin Nikl[c], Akira Yoshikawa[a], Tsuguo Fukuda[a]

[a] *Institute of Multidisciplinary Research for Advanced Materials, Tohoku University, 2-1-1 Katahira, Aoba-ku, Sendai 980-8577 Japan*
[b] *NEC TOKIN Corporation, 28-1 Hanashimashinden, Tsukuba, Ibaraki 305-0875 Japan*
[c] *Institute of Physics ASCR, Cukrovarnicka 10, 16253 Prague, Czech Republic*

**Abstract**

Two-inch size $LiCaAlF_6$ (LiCAF) single crystals doped with $Mg^{2+}$ and $Ba^{2+}$ were successfully grown by the Czochralski technique. Optical absorption measurements in the UV/VIS spectral regions following X-ray irradiation (radiation-induced absorption) were performed in order to investigate the radiation damage of the crystals. It is found that the amplitude of the F-absorption band is suppressed more than a factor of 3 by Mg doping, while in the case of Ba-doped LiCAF, no significant variation is observed. For Mg-doped crystals, the optimum doping concentration is about 0.2 mol% of $Mg^{2+}$. The crystallinity was studied using X-ray rocking curve analysis. The precise measurement of the refractive index showed that refractive index of LiCAF dose not change by the $Mg^{2+}$ doping, within the doping range of $Mg^{2+} < 1.0$ mol%.


*PACS:* 42.88.+h; 78.40.Ha; 78.20.Ci; 81.10.Fq

*Keywords:* A1. F-center; A1. Doping; A1. Induced absorption; A2. Czochralski method; B1. $LiCaAlF_6$; B2. Optical materials

## 1. Introduction

Fluoride single crystals have several advantages as optical materials. Especially their high potential as window materials in the ultra-violet (UV) and vacuum-ultra-violet (VUV) wavelength regions was indicated based on their short wavelength absorption edges [1–3].

Recently, development of VUV wavelength technologies has increased. In particular, an interest in using 157 nm laser source in projection semiconductor lithography as a successor to 193-nm-based systems was announced [4–6]. One of the most serious problems in realizing the 157-nm-based system is the development of suitable optical materials for lenses and other optical components. For an all-refractive design of the 157 nm laser source, a second material other than $CaF_2$ is strongly required. Primary candidates for a second material were LiF and $MgF_2$, however, they have several disadvantages such as a fragile and

*Corresponding author. NEC TOKIN Corporation, 28-1 Hanashimashinden, Tsukuba, Ibaraki 305-0875 Japan. Tel.: +81-22-217-5167; fax: +81-22-217-5102.
*E-mail address:* satohiro@nec-tokin.com (H. Sato).

0022-0248/03/$ - see front matter © 2002 Elsevier Science B.V. All rights reserved.
doi:10.1016/S0022-0248(02)02231-5

hygroscopic nature and large birefringence [7]. Complex fluoride single crystals, such as Colquiriite- and Perovskite-type fluorides, also present many advantages as optical materials, because of their unique properties, such as large band gap. Therefore, we can regard these materials as the candidate.

Window materials in the optical lithography systems must withstand an intense UV/VUV laser irradiation without changing their transmission characteristics. In fluoride crystals, irradiation by X- or gamma-ray or UV light occasionally creates colour centres demonstrating themselves in the appearance of absorption bands in VUV, UV or visible wavelength regions.

Recently, we identified that the $LiCaAlF_6$ (LiCAF) is most resistive material compared with $KMgF_3$ and $BaLiF_3$ by using X-ray [8]. But the absorption band induced by X-ray of LiCAF existed at a wavelength of 262 nm. In the present work, we show how this absorption band can be reduced by doping with aliovalent ions. Since grown crystals have shown superior transmission in the UV and VUV wavelength region, the promising application of them as window materials for optical lithography is also discussed, which we propose as a new, promising material.

## 2. Experimental procedure

Crystal growth was performed in a vacuum-tight Czochralski (CZ) system equipped with an automatic diameter control system. The resistive heater and thermal insulators were made of high-purity graphite. The starting material was prepared from commercial fluoride powders of LiF, $CaF_2$, $AlF_3$ (>99.99%). As a dopant, high-purity $MgF_2$ and $BaF_2$ powders (>99.99%) were used. The melt composition was 5 mol% LiF and $AlF_3$ enriched from the stoichiometric composition, in order to compensate for the vaporization of LiF and $AlF_3$ in the crystal growth process. The concentration of $MgF_2$ and $BaF_2$ in the starting material was from 0.06 to 3.0 mol% ($MgF_2$) and from 0.2 to 3.0 mol% ($BaF_2$). The starting material was placed in a Pt crucible. Vacuum treatment was performed prior to the growth. The system was heated from RT to 700°C for 12 h under vacuum ($\approx 10^{-3}$ Pa). Both rotary and diffusion pumps were used so as to achieve a pressure of $\approx 10^{-3}$ Pa and to effectively eliminate water and oxygen traces from the growth chamber and starting materials. Subsequently, high-purity $CF_4$ gas (99.99%) was slowly introduced into the furnace. Thereafter, the starting material was melted at approximately 820°C. The pulling rate was 0.8 mm/h and the rotation rate was 10 rpm. Growth orientations were controlled using the *a*-axis oriented undoped LiCAF seed crystals. After the growth, the crystals were cooled down to RT at a rate of 30°C/h.

Radiation damage (creating colour centres) has been characterized here by the RT measurement of the radiation-induced optical absorption. The transmission spectrum of the material under study was measured by a Jasco V-530 UV/VIS spectrophotometer in the 190–1000 nm spectral region—before ($T_0$) and immediately after ($T_{irr}$) an irradiation procedure and the induced absorption

$$\mu(\lambda) = \ln\left(T_0(\lambda)/T_{irr}(\lambda)\right) \quad (1)$$

was calculated. It should be taken into account that the samples have high absorption coefficient against X-ray. It is typically achieved in LiCAF below 1 mm thickness using standard attenuation calculation according to Ref. [9]. In order to compare, all the samples were prepared with the same thickness of about 2 mm. Irradiation was accomplished by an X-ray tube (25 kV, Rigaku diffractometer). In the case of the induced absorption measurements, subsequent irradiation doses were set at 240 Gy.

The crystal quality of the undoped, Mg- and Ba-doped LiCAF single crystals, corresponding to the width of the peak, characterized by X-ray rocking curve (XRC) measurement using RIGAKU ATX-E with a 4-bounce Ge (2 2 0) channel-cut monochromator. In order to obtain correct FWHM values from $\varpi$ scan profile measurements, selection appropriate X-ray optics with respect to the sample quality is necessary. In our set-up, the beam divergence was 0.003°. CuK$\alpha_1$ X-ray source ($\lambda = 1.54056$ Å) was used, and $\varpi$ scans were carried out.

The refractive indices of undoped and 1.0 mol% Mg-doped LiCAF crystals were measured accurately down to five decimal places. Both LiCAF crystals were cut in the shape of a dispersion prism, 60° and 20 mm on each side, and polished. The measurement was performed at different 13 wavelengths from 148.2826 to 202.613 nm with the minimum deviation method using MOLLER-WEDEL goniometer-spectrometer (type 1 UV-VIS-IR). The refractive indices were measured for different polarized light to the *c*-axis of the crystal, parallel and vertical, respectively ($n_e$, $n_0$). The measurement was performed under $N_2$ atmosphere at a pressure of 1013.3 hPa and temperature was controlled between 25.0°C and 25.1°C. The precision was $\pm 2 \times 10^{-5}$ in this measurement.

## 3. Results and discussion

Fig. 1 shows as-grown 3.0 mol% Mg-doped- and Ba-doped-LiCAF single crystals with 2 in (50 mm) in diameter and 150 mm in length. As it can be seen, many inclusions occurred in both crystals. This is because the difference of the charge and ionic radius. Fig. 2 shows as-grown 1.0 mol% Mg-doped and Ba-doped-LiCAF single crystals with 2 in (50 mm) diameter. There are no

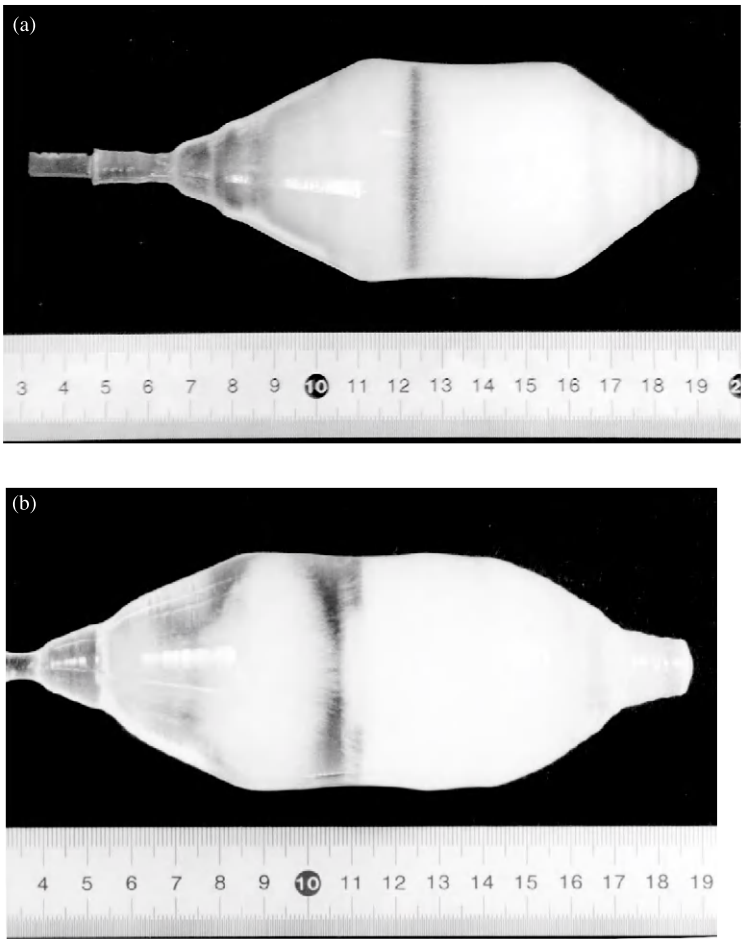


Fig. 1. As-grown 3.0 mol% Mg-doped (a) and Ba-doped (b) $LiCaAlF_6$ crystals 2 in diameter. There are visible inclusions at the bottom.

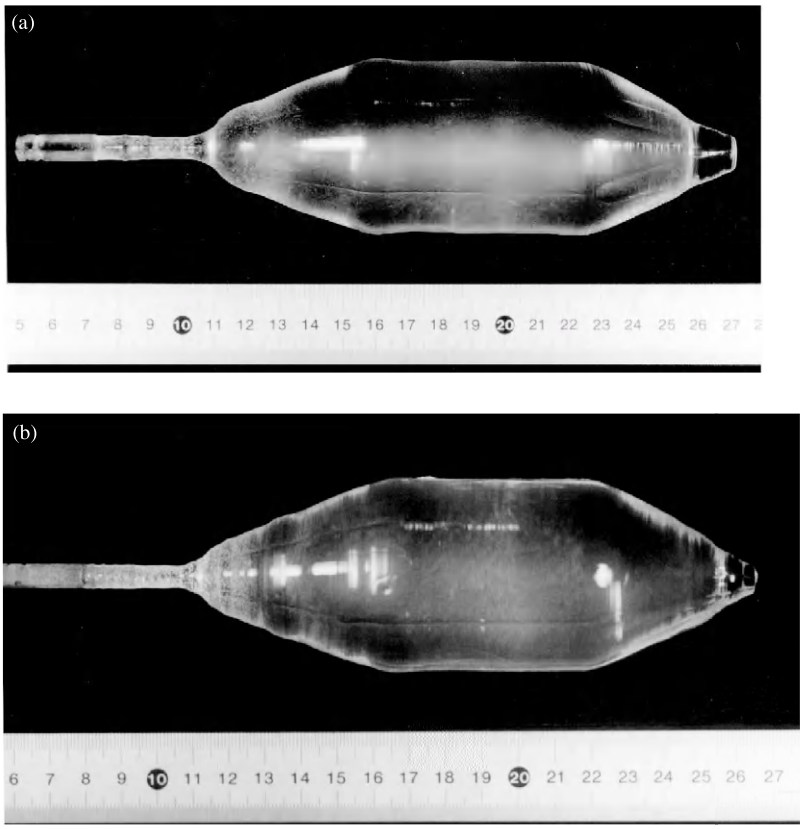


Fig. 2. As-grown 1.0 mol% Mg-doped (a) and Ba-doped (b) $LiCaAlF_6$ crystals 2 in diameter without inclusions.

visible inclusions and cracks. Based on these results, LiCAF single crystals doped with $Mg^{2+}$ or $Ba^{2+}$ of less than 1.0 mol% was selected to grow and characterized.

Recently, we identified that it is reasonable to ascribe the band at 262 nm in LiCAF to an F-centre [10]. Therefore, we considered the possibility of decreasing the F-centre concentration in LiCAF crystal. This can be achieved by reducing the concentration of fluorine vacancies, which is considered as an intrinsic problem for undoped LiCAF crystal. A simple coulombic equilibrium-based approach consists in the increase of a positive charge in the crystal (e.g. by doping with substitutional ions with a higher positive valency), which would inhibit (or at least decrease) the formation of fluorine vacancies during the crystal growth. An important requirement is that such doping should not create any other trap level within the forbidden gap of the crystal. There are many possibilities in the LiCAF structure due to three available cationic sites. As the most feasible, doping with divalent ions at the Li site was considered. In order to limit the occupation of $Ca^{2+}$ sites by divalent dopants, one must choose an ion with a size similar to that of Li. The most stable divalent ions are those from the alkaline-earth metal group and among them, the $Mg^{2+}$ ion satisfactorily fits to the Li size. Moreover, $Mg^{2+}$ is known not to create any trap levels within the $CaF_2$ forbidden gap [11,12], so that Mg doping was finally chosen. To test the importance of the ionic size, $Ba^{2+}$ doping was tried as well, since $Ba^{2+}$ ions are approximately twice as large as $Li^{+}$ ones, so the probability of their occurrence at the Li site in LiCAF is negligible.

Fig. 3(a) shows the induced absorption for the undoped, 0.2 mol% Mg-doped and 0.2 mol%

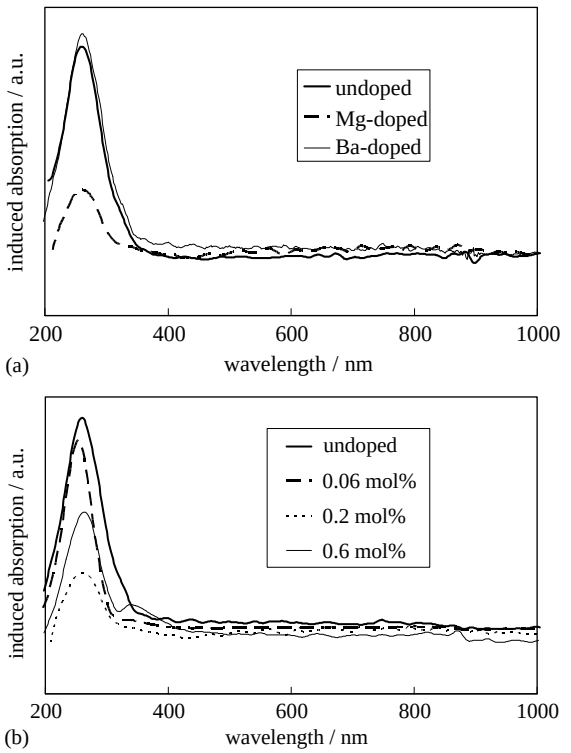


Fig. 3. Induced absorption after X-ray irradiation; (a) undoped, 0.2 mol% Mg and 0.2 mol% Ba-doped $LiCaAlF_6$ crystals, (b) undoped, 0.06, 0.2 and 0.6 mol% Mg-doped $LiCaAlF_6$ crystals.

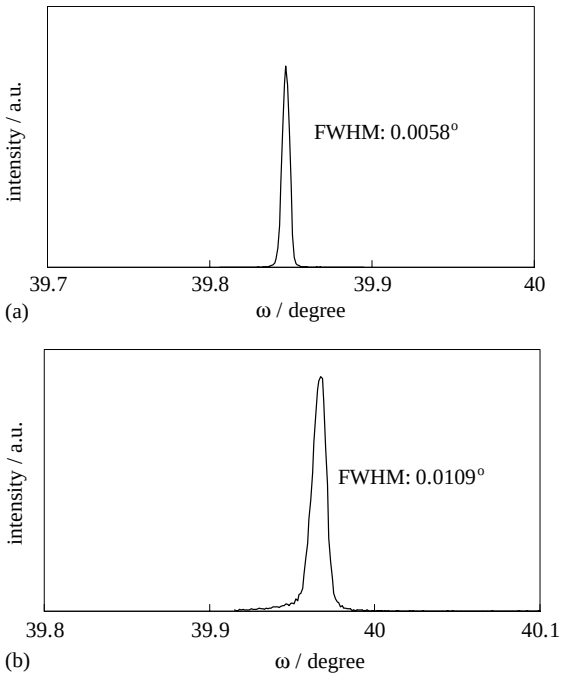


Fig. 4. XRC (ϖ scan) of $LiCaAlF_6$ (008) single crystal; (a) undoped $LiCaAlF_6$ crystal, (b) 0.2 mol% Mg-doped $LiCaAlF_6$ crystal.

Ba-doped-LiCAF crystals after a cumulative dose of 240 Gy. As can be seen, the amplitude of the F-absorption band decreases compared to undoped one, while no significant change is obtained for the Ba-doped LiCAF. The amplitude of induced absorption at 262 nm for the undoped and Mg-doped (0.06, 0.2 and 0.6 mol% in melt) LiCAF are shown in Fig. 3(b). It can be noted that the amplitude of the F-absorption band is getting lower by more than a factor of 3 in the Mg-doped LiCAF (0.2 mol%) compared to undoped, from the data given in Fig. 3(b). It can be deduced that best $MgF_2$ doping concentration is about 0.2 mol% in the melt.

It is worth noting that the present study does not provide any detailed information about the sites responsible for positive charge localization, i.e. about the hole centres stable at RT. Since radiation damage is a result of simultaneous and separate localization of electrons and holes in the lattice, the final level of the damage obtained is limited by the capacity of the material to localize both positive and negative charge carriers.

The crystal quality of the grown crystal was characterized by XRC measurements. ϖ scan has carried out for the reflection from (0 0 8) plane corresponding to the ⟨0 0 1⟩ direction. The spectra for undoped- and 1.0 mol% Mg-doped-LiCAF crystal are shown in Fig. 4. It is shown that the FWHM was measured to be 0.0058° and 0.0109°. According to the results of measurements, the sample studied has as high crystallinity as that of other optical grade materials.

Fig. 5 shows prepared prisms for the measurement of refractive indices. The coefficients of Sellmeier equations as shown below for undoped- and 1.0 mol% Mg-doped-LiCAF crystals were calculated from measured 13 refractive indices by the least-square method, respectively. Table 1 shows calculated coefficients from the Sellmeier equation for undoped- and 1.0 mol% Mg-doped-

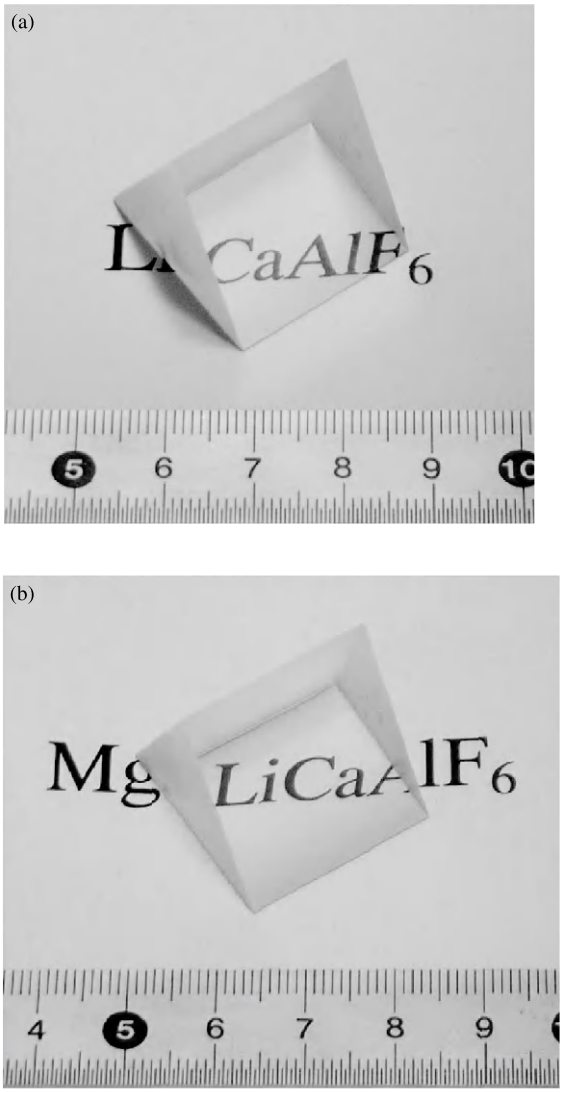


Fig. 5. Undoped (a) and 1.0 mol% Mg-doped (b) $LiCaAlF_6$ prism prepared for the precise measurements of refractive indices.

LiCAF single crystals

$$n^2 = A_0 + A_1\lambda^2 + A_2\lambda^{-2} + A_3\lambda^{-4} + A_4\lambda^{-6} + A_5\lambda^{-8} + A_6\lambda^{-10}. \quad (2)$$

Fig. 6 shows refractive indices measured depending on wavelength, together with lines calculated from the Sellmeier equation for LiCAF, Eq. (2). The results showed that the difference of the refractive index between undoped- and 1.0 mol% Mg-doped-LiCAF was less than 0.00002 at all the measured wavelengths. As this difference was same as the measurement precision, it can be considered that the refractive index of LiCAF does not change by doping with $Mg^{2+}$ in the case of less than 1.0 mol%.

Table 1
Calculated coefficients from the Sellmeier equation for undoped and 1.0 mol% Mg-doped $LiCaAlF_6$ single crystals

| | undoped $LiCaAlF_6$ | | 1.0 mol% Mg-doped $LiCaAlF_6$ | |
|---|---|---|---|---|
| | $n_e$ | $n_0$ | $n_e$ | $n_0$ |
| $A_0$ | 1.91103 | 1.940094 | 1.925154 | 1.907119 |
| $A_1$ | −0.09594 | −0.09433 | −0.09521 | −0.09610 |
| $A_2$ | 0.006003 | 0.001283 | 0.003678 | 0.006769 |
| $A_3$ | $-8.4\times10^{-5}$ | 0.000188 | $-3.75\times10^{-5}$ | $-1.39\times10^{-4}$ |
| $A_4$ | $4.49\times10^{-6}$ | $-3.2\times10^{-6}$ | $1.49\times10^{-6}$ | $6.39\times10^{-6}$ |
| $A_5$ | $-7.1\times10^{-8}$ | $3.67\times10^{-8}$ | $-3.46\times10^{-8}$ | $-1.02\times10^{-7}$ |
| $A_6$ | $5.43\times10^{-10}$ | $-4.5\times10^{-11}$ | $3.84\times10^{-10}$ | $7.44\times10^{-10}$ |

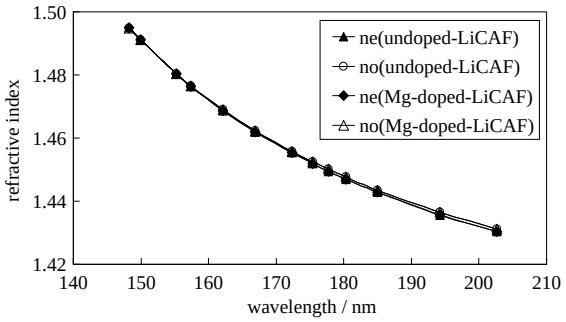


Fig. 6. Refractive indices of undoped and 1.0 mol% Mg-doped $LiCaAlF_6$ single crystals depending on wavelength.

## 4. Conclusion

Two-inch size $LiCaAlF_6$ (LiCAF) single crystals undoped and doped with $MgF_2$ and $BaF_2$ were successfully grown by the Czochralski technique under a $CF_4$ atmosphere. Mg doping decreases the amplitude of the F-centre absorption band and the optimum doping concentration turns to be about 0.2 mol% of $MgF_2$ in the melt. It is proposed that $Mg^{2+}$ partly occupies Li sites. Thus, it introduces

an excessive positive charge in the cation sublattice, which can reduce the concentration of fluorine vacancies in the process of crystal growth and consequently the concentration of F-centres after an X-ray irradiation. The inefficiency of $Ba^{2+}$ doping in the suppression of F centres can consistently be explained by taking into account its larger ionic radius, so that the probability of its occurrence at Li sites is negligible. From the XRC measurement, the FWHM values show that the undoped and Mg-doped-LiCAF crystals have as high crystallinity as other optical grade crystals. Precise measurement of the refractive indices for undoped and Mg-doped-LiCAF shows that Refractive index of LiCAF does not change by doping with $Mg^{2+}$ in the case of less than 1.0 mol%.

## Acknowledgements

The authors would like to thank Mr. Murakami, of the Laboratory for Developmental Research of Advanced Materials in Institute for Materials Research, for his assistance with the X-ray irradiation. This research was partially supported by a Scientific Research Grant-in-Aid from the New Energy and Industrial Technology Development Organization (NEDO).

## References

[1] K. Shimamura, S.L. Baldochi, N. Mujilatu, K. Nakano, Z. Liu, N. Sarukura, T. Fukuda, J. Crystal Growth 211 (2000) 302.
[2] K. Shimamura, T. Fujita, H. Sato, A. Bensalah, N. Sarukura, T. Fukuda, Jpn. J. Appl. Phys. 39 (2000) 6807.
[3] A. Bensalah, K. Shimamura, K. Nakano, T. Fujita, T. Fukuda, J. Crystal Growth 231 (2001) 143.
[4] R. Harbison, Proceedings of the First International Symposium157 nm Lithography, California, USA, Vol. 1, 2000, p. 9.
[5] S.M. Hooker, P.T. Landsberg, Prog. Quantum Electron. 18 (1994) 227.
[6] M.D. Whitfield, S.P. Lansley, O. Gaudin, R.D. McKeag, N. Rizvi, R.B. Jackman, Diamond Relat. Mater. 10 (2001) 693.
[7] T.M. Bloomstein, M.W. Hom, M. Rothschild, R.R. Kunz, S.T. Palmacol, R.B. Goodman, J. Vac. Sci. Technol. B 15 (1997) 2112.
[8] H. Sato, K. Shimamura, A. Bensalah, N. Solovieva, A. Beitlerova, A. Vedda, M. Martini, H. Machida, T. Fukuda, M. Nikl, Jpn. J. Appl. Phys. 41 (2002) 2028.
[9] F.H. Attix, W.C. Roesch (Eds.), Radiation Dosimetry, Vol. 1, Academic Press, New York, 1968, pp. 112–144 (Chapter 4).
[10] H. Sato, K. Shimamura, A. Bensalah, T. Satonaga, E. Mihokova, M. Dusek, A. Vedda, M. Martini, H. Machida, T. Fukuda, M. Nikl, J. Appl. Phys. 91 (2002) 5666.
[11] V. Denks, A. Maaroos, V. Nagirnyi, T. Savikhina, V. Vassiltsenko, J. Phys: Condens. Matter 11 (1999) 3115.
[12] V.M. Bermudez, Solid State Commun. 118 (2001) 569.